The ISW seen by Planck

P. Vielva, on behalf of the Planck Collaboration

Cosmology and Fundamental Physics with Planck @ CERN, 19th June 2013

ISW is a weak signal!

~ 3σ → "detection"

1. **The ISW effect**

2. **The ISW in Planck**

3. **Future steps**

4. **Conclusions**

- **The physics of the ISW effect**
- **The ISW detection**
  - **Expected S2N**
  - **Cross-correlation with LSS tracers**
  - **The ISW-lensing bispectrum**

- **The physics of the ISW effect**

- **The ISW detection**
  - **Expected S2N**
  - **Cross-correlation with LSS tracers**
  - **The ISW-lensing bispectrum**

The physics of the ISW effect

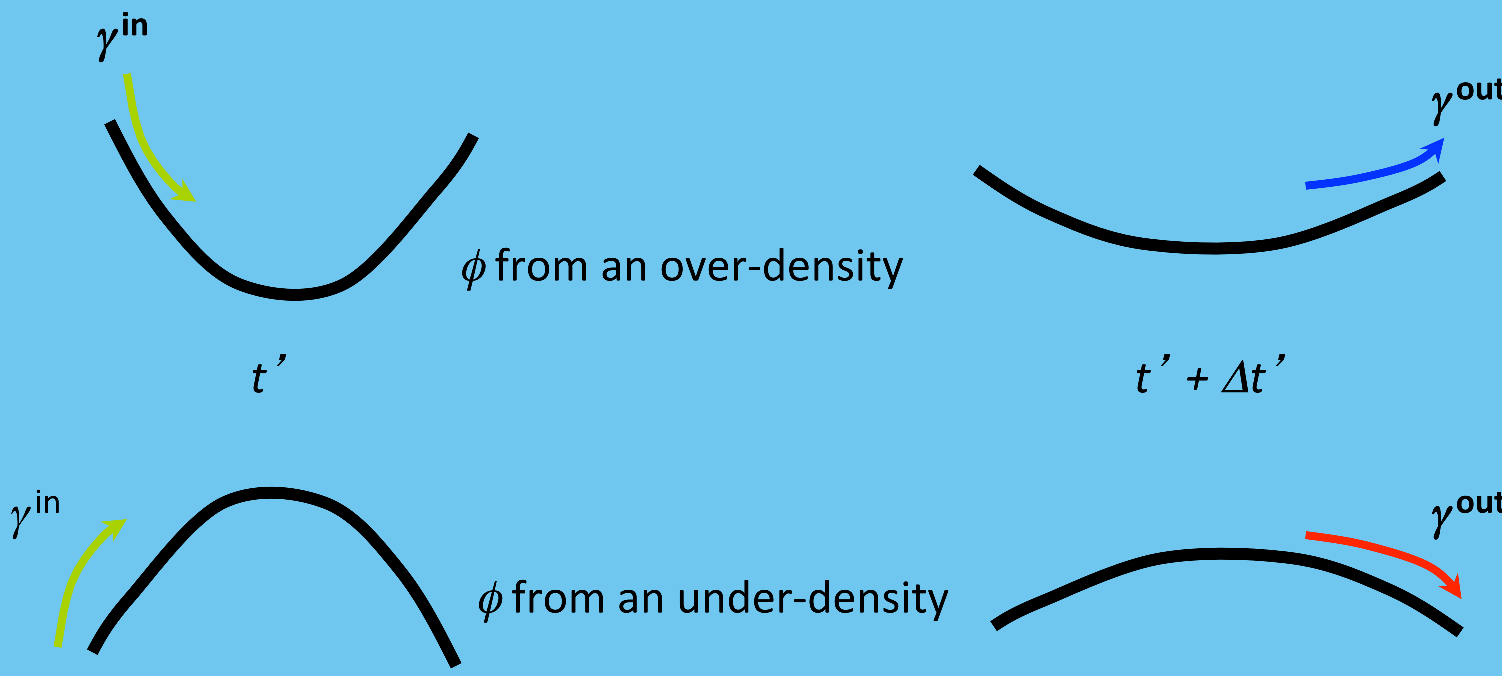

- CMB photons are blue (red) shifted when fall into (out of) gravitational potential wells
- An **evolution of the gravitational potential** during the photon crossing implies a **net change in the photon energy** ➔ **secondary anisotropy of the CMB anisotropies**

The physics of the ISW effect

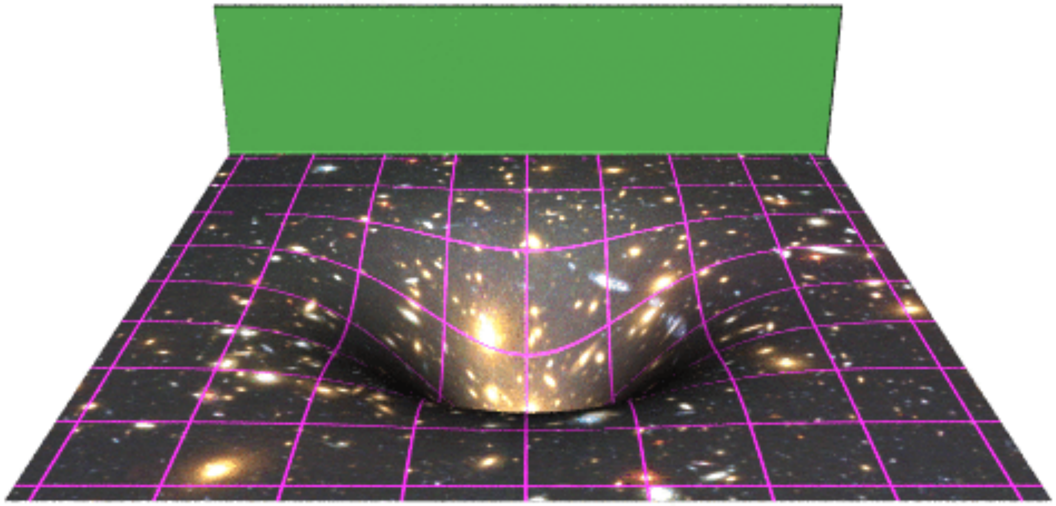

[Granett et al.]

- CMB photons are blue (red) shifted when fall into (out of) gravitational potential wells
- An **evolution of the gravitational potential** during the photon crossing implies a **net change in the photon energy** ➔ **secondary anisotropy of the CMB anisotropies**

IFCA Instituto de Física de Cantabria

The physics of the ISW effect

• In a matter dominated (Einstein-De Sitter) universe, the gravitational potentials remain constant w.r.t. the conformal time ➔ no net ISW signal.

• Hence, the detection of the ISW effect can be related to the presence of a given curvature (e.g., Kaminkowski & Spergel 1994) or a **dark energy component** (e.g., Crittenden & Turok 1996) governing the expansion.

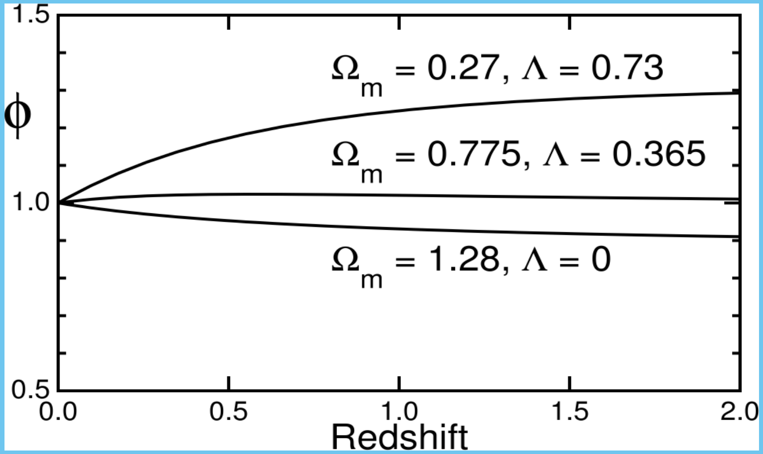

$$\frac{\Delta T}{T_0}(\vec{n}) = -2\int_0^{\eta_{\rm dec}} d\eta \frac{d\phi}{d\eta}(\eta\vec{n})$$

[Nolta et al., 2004]

• Other effects modifying the properties of the gravitational potential with time, might introduce, as well, an ISW effect. In particular, the ISW could be used **to explore modified gravity theories** (e.g., Hu 2002)

- The physics of the ISW effect
- **The ISW detection**
  - Expected S2N
  - Cross-correlation with LSS tracers
  - The ISW-lensing bispectrum

The ISW detection: expected s2n

Unfortunately, the **ISW contribution to the CMB anisotropies is subdominant**: it is covered by the primordial fluctuations at very large scale.

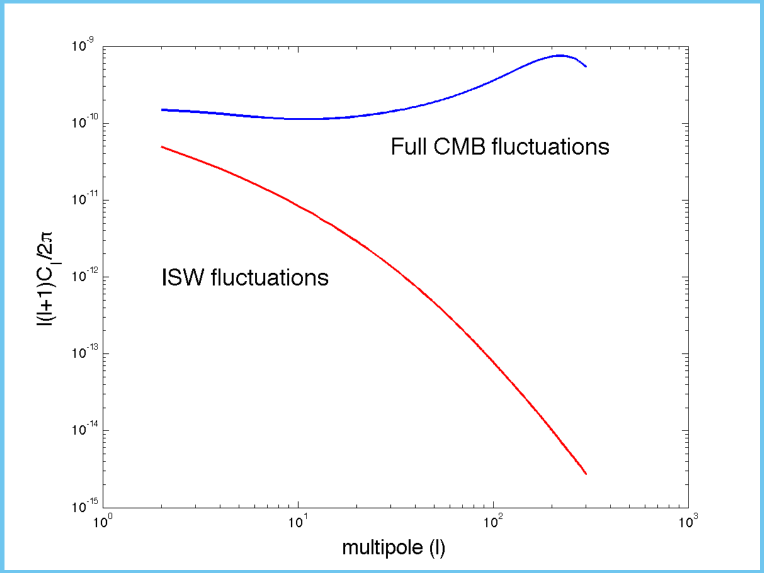

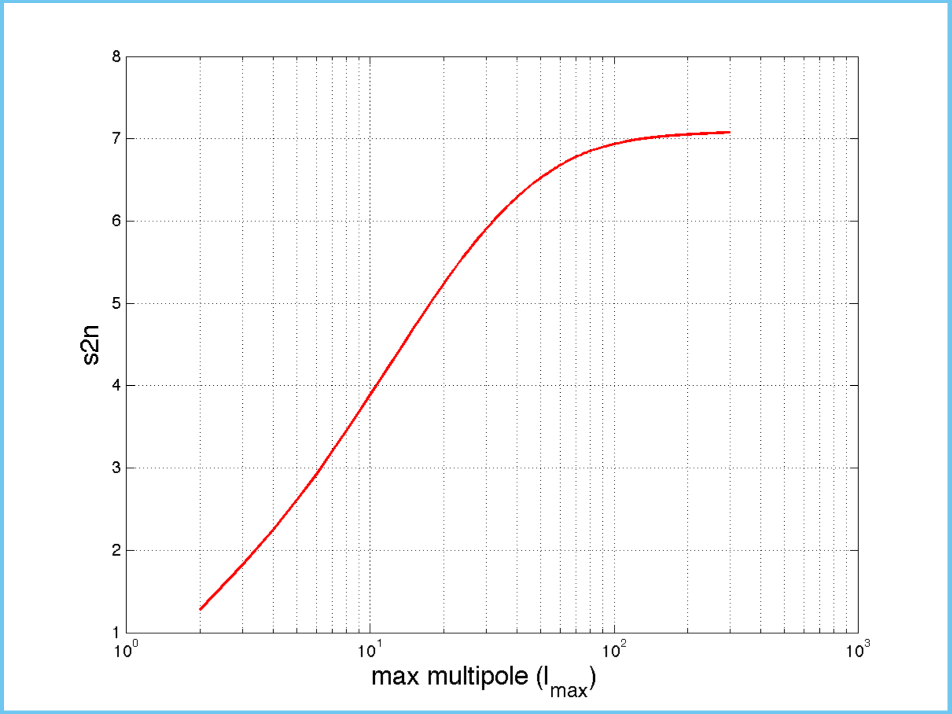

It can be detected, however, by cross-correlating the CMB fluctuations with a tracer of the matter distribution (e.g., Crittenden & Turok 1996) ➔ a **maximum of 7σ** is expected from a **perfect tracer**.

The ISW detection: cross-correlation with LSS tracers

However, actual tracers (as galaxy catalogue surveys) are far from being ideal tracers:

$$X_\ell = 12\pi\Omega_m H_0^2 \int \frac{dk}{k^3} \Delta_\delta^2(k) F_\ell^T(k) F_\ell^G(k)$$

Approximate estimation of the ISW s2n detection via the cross-correlation with a LSS tracer, as a function of:

- Survey properties
- Full covariance

$$\left(\frac{S}{N}\right)_{ISW}^2 \approx \sum_{\ell=2}^{\ell_{\max}} (2\ell+1) \frac{X_\ell^2}{X_\ell^2 + T_\ell \left(G_\ell + \frac{1}{\bar{n}}\right)} f_{sky}$$

The ISW detection: cross-correlation with LSS tracers

However, actual tracers (as galaxy catalogue surveys) are far from being ideal tracers:

- **Incomplete sky** coverage (also on the CMB side) ➔ increase **sampling variance**

$$\left(\frac{S}{N}\right)^2_{ISW} \approx \sum_{\ell=2}^{\ell_{\max}} (2\ell+1) \frac{X_\ell^2}{X_\ell^2 + T_\ell\left(G_\ell + \frac{1}{\bar{n}}\right)} \boxed{f_{sky}}$$

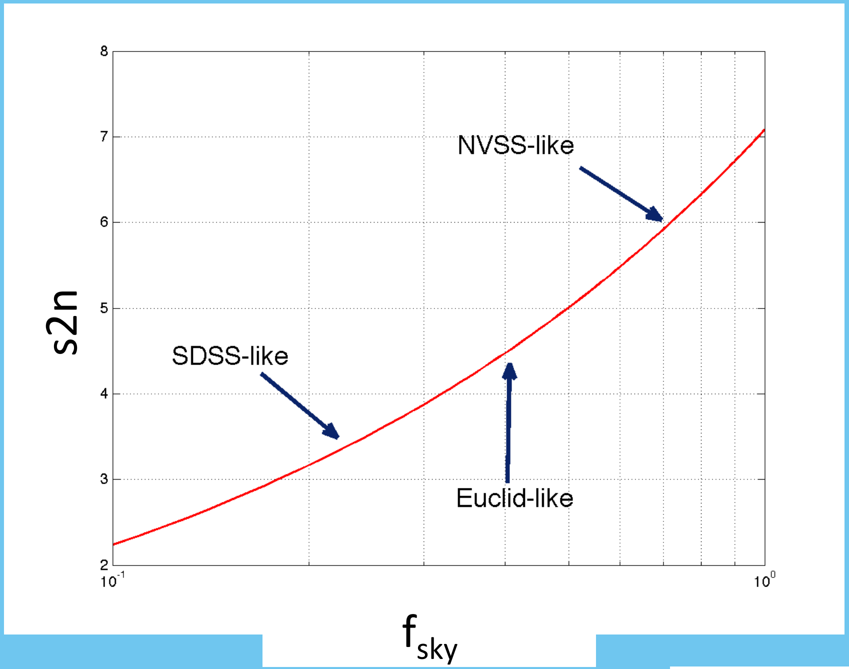

P. Vielva

IFCA Instituto de Física de Cantabria

The ISW detection: cross-correlation with LSS tracers

However, actual tracers (as galaxy catalogue surveys) are far from being ideal tracers:

- **Incomplete sky** coverage (also on the CMB side) ➔ increase **sampling variance**
- **Finite number of counts** ➔ **extra noise** on the gravitational potential description

$$\left(\frac{S}{N}\right)^2_{ISW} \approx \sum_{\ell=2}^{\ell_{max}} (2\ell+1) \frac{X_\ell^2}{X_\ell^2 + T_\ell \left(G_\ell + \frac{1}{\boxed{\bar{n}}}\right)} f_{sky}$$

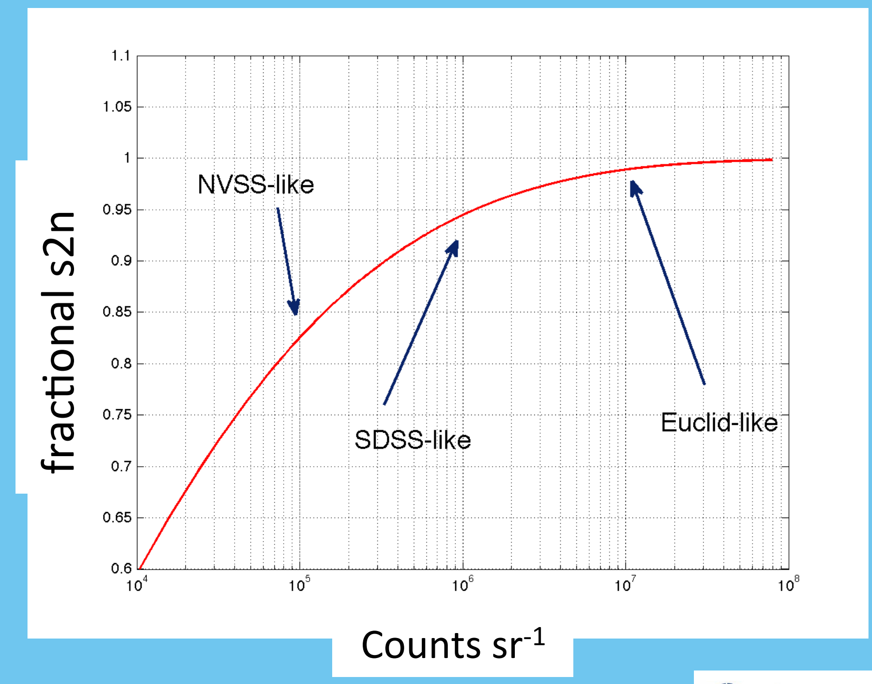

P. Vielva
IFCA Instituto de Física de Cantabria

The ISW detection: cross-correlation with LSS tracers

However, actual tracers (as galaxy catalogue surveys) are far from being ideal tracers:

- **Incomplete sky** coverage (also on the CMB side) ➔ increase **sampling variance**
- **Finite number of counts** ➔ **extra noise** on the gravitational potential description
- **Reduced redshift range** ➔ **incomplete mapping** of the gravitational potential

[Afshordi 2004]

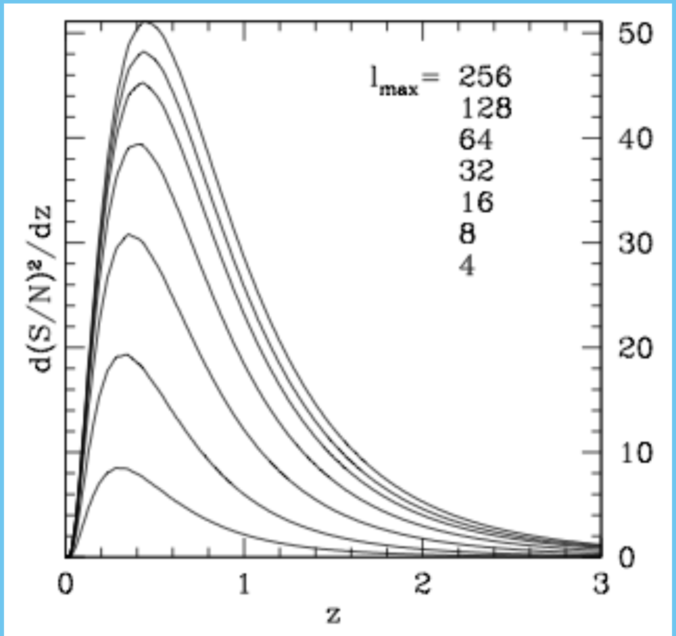

$$\left(\frac{S}{N}\right)^2_{ISW} \approx \sum_{\ell=2}^{\ell_{max}} (2\ell+1) \frac{\boxed{X_\ell^2}}{\boxed{X_\ell^2} + T_\ell\left(\boxed{G_\ell} + \frac{1}{\bar{n}}\right)} f_{sky}$$

The ISW detection: cross-correlation with LSS tracers

However, actual tracers (as galaxy catalogue surveys) are far from being ideal tracers:

- **Incomplete sky** coverage (also on the CMB side) ➔ increase **sampling variance**
- **Finite number of counts** ➔ **extra noise** on the gravitational potential description
- **Reduced redshift range** ➔ **incomplete mapping** of the gravitational potential

It was in 2004, [Boughn and Crittenden] when the **first detection of the ISW effect was claimed**, by cross-correlating the WMAP CMB signal with HEAO-1 and NVSS.

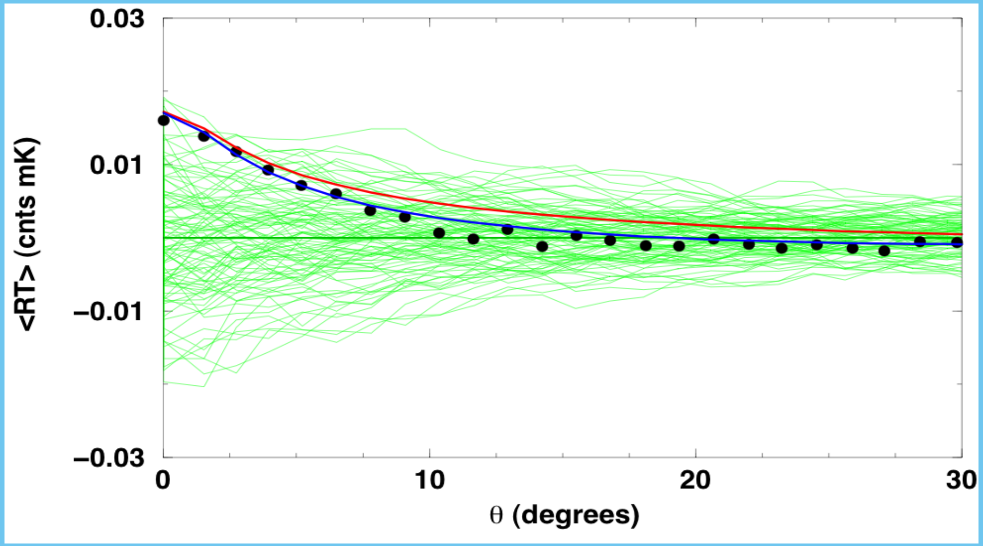

$\sim 2.5\sigma$

P. Vielva
IFCA Instituto de Física de Cantabria

The ISW detection: cross-correlation with LSS tracers

Afterwards, **tens of works have explored the ISW** by cross-correlating WMAP with several LSS surveys.

An almost complete list:

ISW effect through correlations with tracer catalogues: 2MASS (an infrared catalogue at low redshifts around 0.1, Afshordi et al. 2004; Dupé et al. 2011; Francis & Peacock 2009; Rassat et al. 2006), *HEAO* (an X-ray survey at low redshift, with the first positive claim for detection, Boughn & Crittenden 2004), Sloan Digital Sky Survey (SDSS, optical survey at intermediate redshifts, Bielby et al. 2010; Cabré et al. 2006; Fosalba et al. 2003; Fosalba & Gaztañaga 2004; Giannantonio et al. 2006; Granett et al. 2009; López-Corredoira et al. 2010; Padmanabhan et al. 2005; Sawangwit et al. 2010; Scranton et al. 2003; Xia 2009), the NRAO VLA Sky Survey (NVSS, radio catalogue with high-redshift sources, Boughn & Crittenden 2005; Hernández-Monteagudo 2010; Massardi et al. 2010; McEwen et al. 2007; Pietrobon et al. 2006a; Raccanelli et al. 2008; Schiavon et al. 2012; Vielva et al. 2006), and combined measurements with multiple tracers (Corasaniti et al. 2005; Gaztañaga et al. 2006; Giannantonio et al. 2008, 2012; Ho et al. 2008; Nolta et al. 2004). The significance of the ISW detections that can be found

Results are diverse: from no detection up to 4.7σ claims.

One of the most important reasons for the differences is the **different nature of the detection tests applied on each work**.

The ISW detection: the ISW-lensing bispectrum

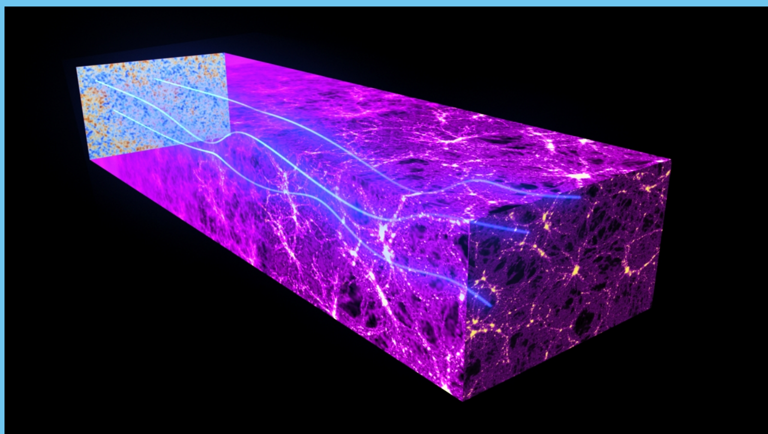

$$B^{m_1 m_2 m_3}_{\ell_1 \ell_2 \ell_3} \equiv \langle a_{\ell_1 m_1} a_{\ell_2 m_2} a_{\ell_3 m_3} \rangle = \langle a^{\mathrm{P}}_{\ell_1 m_1} a^{\mathrm{L}}_{\ell_2 m_2} a^{\mathrm{ISW}}_{\ell_3 m_3} \rangle + 5 \text{ perm.}$$

$$B^{m_1 m_2 m_3 \,(\mathrm{ISW-L})}_{\ell_1 \ell_2 \ell_3} = \mathcal{G}^{m_1 m_2 m_3}_{\ell_1 \ell_2 \ell_3} b^{\mathrm{ISW-L}}_{\ell_1 \ell_2 \ell_3}$$

$$b^{\mathrm{ISW-L}}_{\ell_1 \ell_2 \ell_3} = \frac{\ell_1(\ell_1+1) - \ell_2(\ell_2+1) + \ell_3(\ell_3+1)}{2} \times \tilde{C}^{\mathrm{TT}}_{\ell_1} C^{\mathrm{T}\phi}_{\ell_3} + (5 \text{ perm.}) \,.$$

The **CMB lensing and the ISW are correlated**: both are caused by the same matter gravitational potential. Planck provides the **first opportunity** to probe such correlation (**Expected s2n = 3.3σ**)

It induces **a non-zero bispectrum** of the CMB fluctuations, with a "squeezed" configuration: one short leg at low multipole (ISW) and two small scale modes at high multipole associated to the lensing induced correlation ➔ **non-negligible bias to the primordial local f_{NL}**.

- **The data**
    - **Planck CMB maps**
    - **Planck lensing map**
    - **External LSS tracers**

- **The ISW detection with Planck**
    - **ISW-lensing**
    - **Cross-correlation with LSS tracers**
    - **Stacking on the position of large structures**

- **The ISW map recovery**

- **The data**
  - **Planck CMB maps**
  - **Planck lensing map**
  - **External LSS tracers**
- **The ISW detection with Planck**
  - **ISW-lensing**
  - **Cross-correlation with LSS tracers**
  - **Stacking on the position of large structures**
- **The ISW map recovery**

Instituto de Física de Cantabria

The data: Planck CMB maps

Planck has produced **4 different clean CMB maps** out of different component separation pipelines: Commander-Ruler (**parametric in real space**, SNR=1 @ l=1550), NILC (**non-parametric in wavelet space**, SNR=1 @ l =1790), SEVEM (**non-parametric in real space**, SNR=1 @ l=1790) and SMICA (**semi-parametric in harmonic space**, SNR=1 @ l=1790)

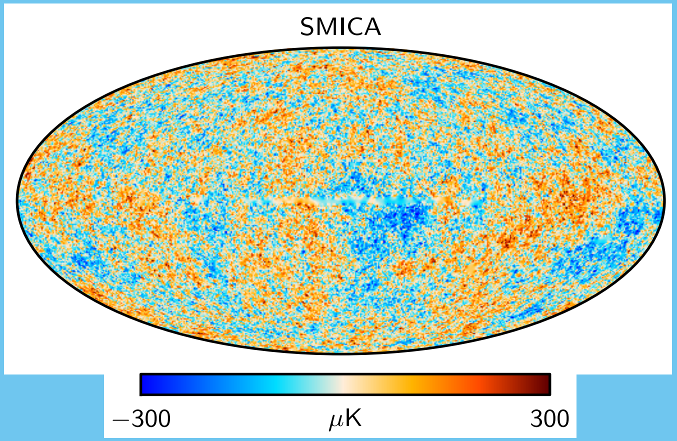

These 4 maps have been used in the ISW analyses, as **a check of robustness**. Depending on the performed analyses, **different resolutions** have been considered:

- Full resolution (~5 arcmin) ➔ ISW-lensing bispectrum
- Intermediate resolution (~30 arcmin) ➔ stacking
- Low resolution (> 1 degree) ➔ ISW-LSS correlation and the ISW map recovery

In addition, **specific clean CMB maps at several frequencies** (44, 70, 100, 143, 217 and 353 GHz) were produced by **SEVEM** to study the cosmological nature of the stacked signals.

The data: Planck lensing map

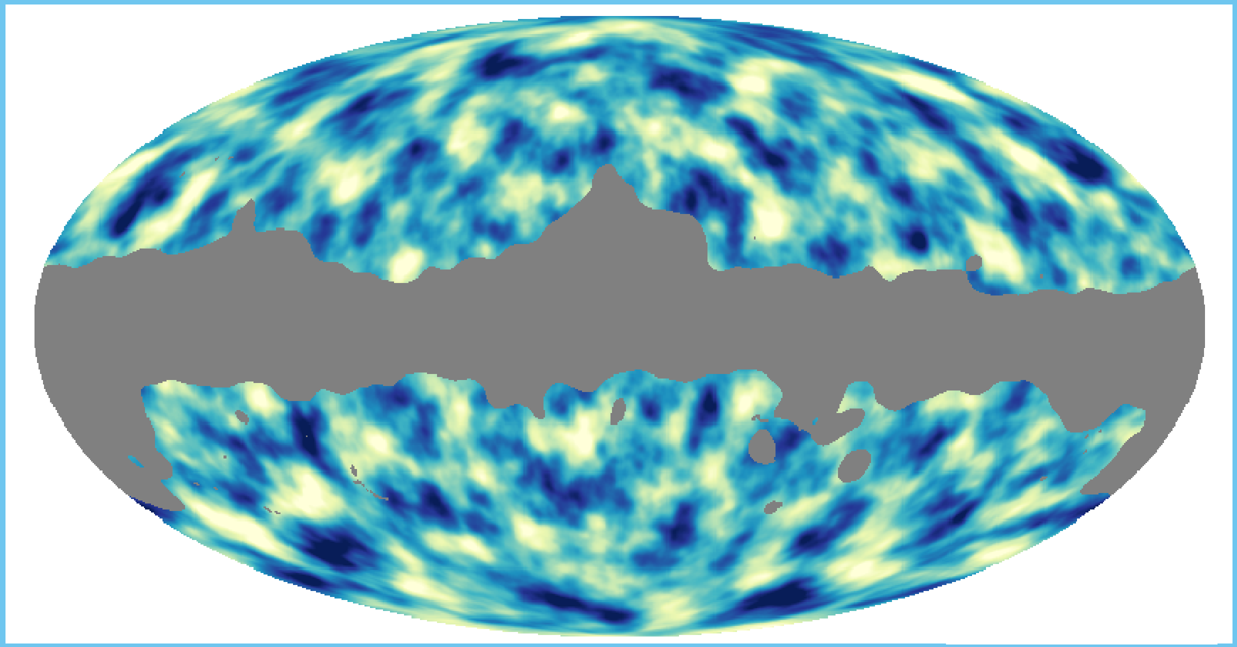

This Planck lensing map has been used as an alternative template to study **the ISW-lensing bispectrum** via the direct CMB and lensing cross-correlation.

It is also used to **infer the ISW map** fluctuations caused by this potential field.

The data: external LSS tracers

Three galaxy surveys catalogues have been used as tracers of the LSS.

NVSS

Radio catalogue:

- f_{sky} = 0.73
- Mean redshift = 1.17
- 1.6x10^5 counts per stereoradian

Expected s2n = 3.0

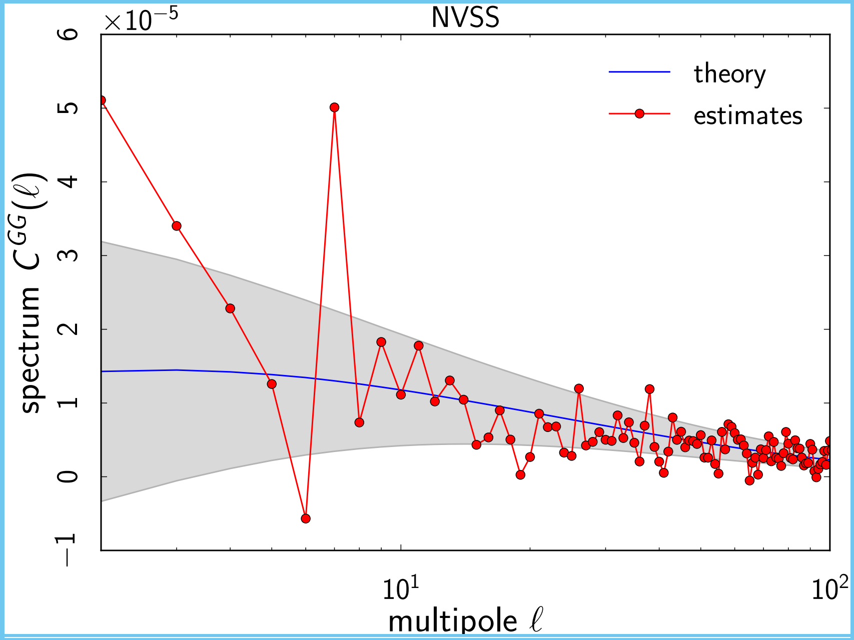

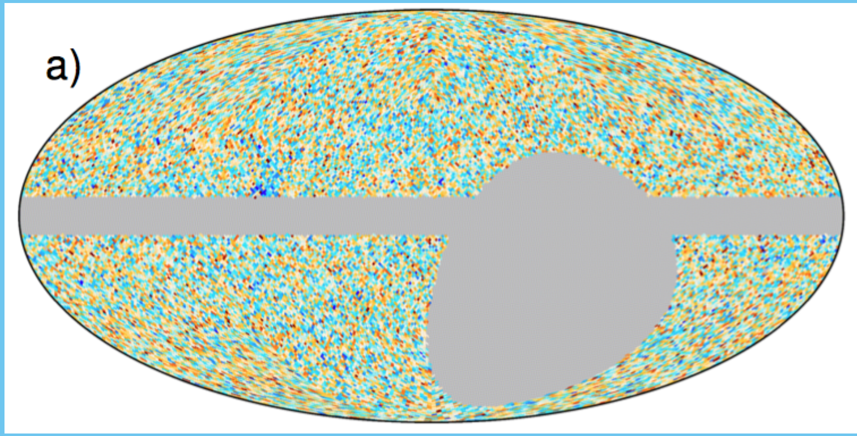

The data: external LSS tracers

Three galaxy surveys catalogues have been used as tracers of the LSS.

SDSS Luminous Galaxies

Optical catalogue:

- f_{sky} = 0.22
- Mean redshift = 0.45
- 5.6x10^5 counts per stereoradian

Expected s2n = 1.9

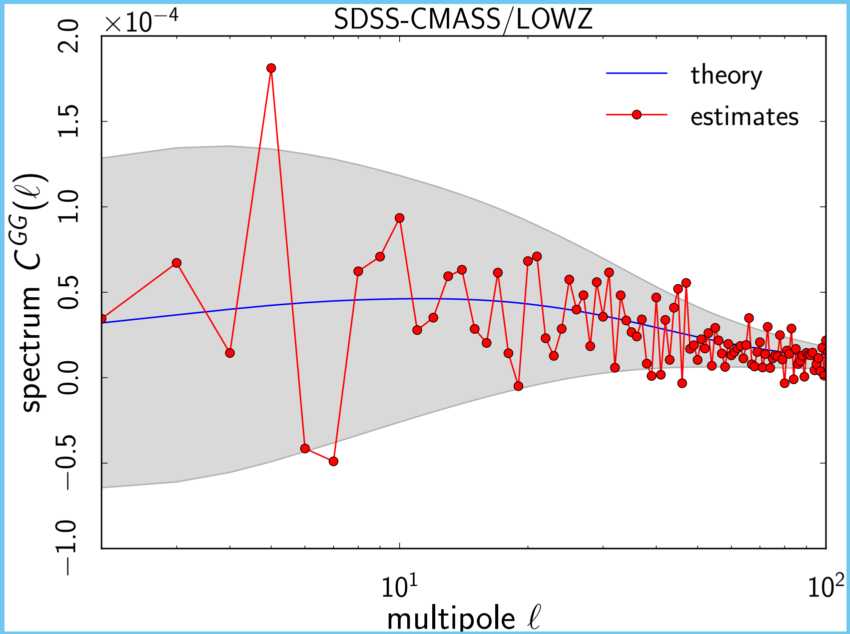

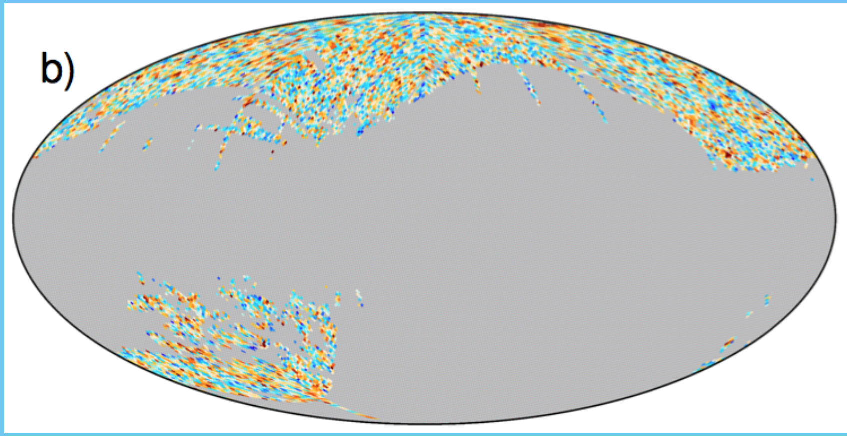

The data: external LSS tracers

Three galaxy surveys catalogues have been used as tracers of the LSS.

SDSS Main Galaxies

Optical catalogue:

- $f_{sky} = 0.22$
- Mean redshift = 0.32
- 9.7×10^6 counts per stereoradian

Expected s2n = 0.6

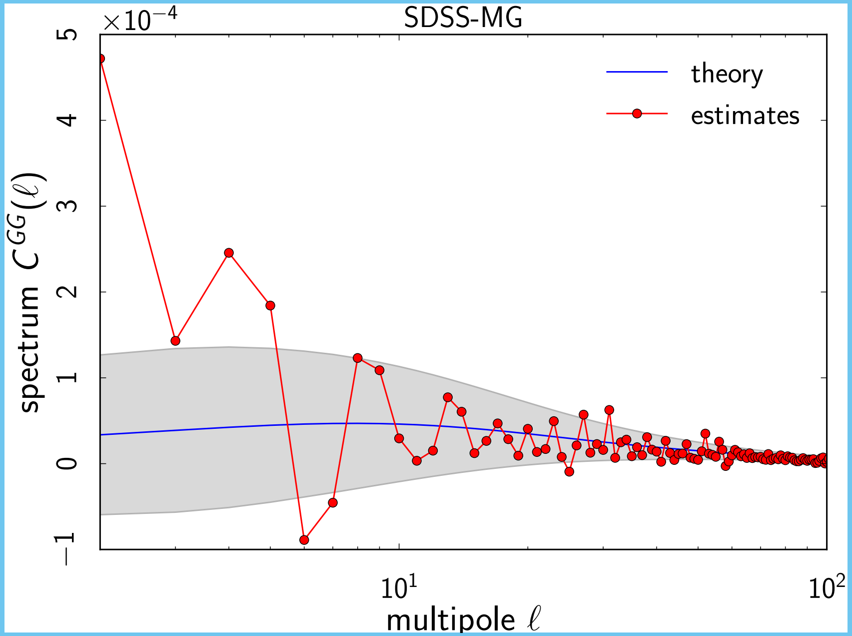

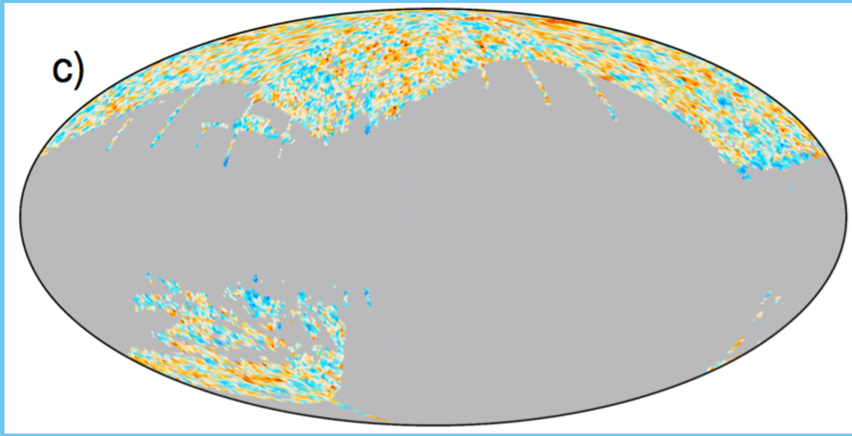

The data: external LSS tracers

Additionally, **clusters and voids catalogues** have been used to **study** in detail the **CMB fluctuations on the position of these structures**. All these catalogues are based on SDSS data:

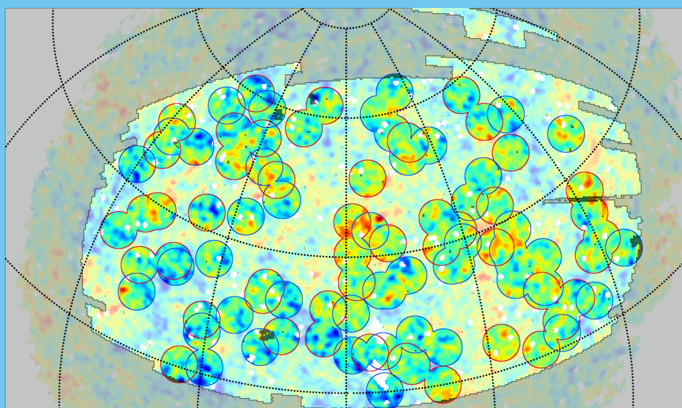

Grannet et al.

50 clusters
50 voids

0.4 < z < 0.75

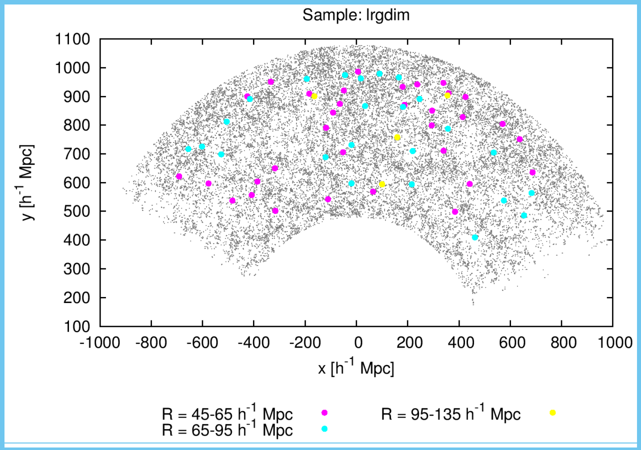

Sutter et al.

0 < z < 0.44

1495 voids

- The data
  - Planck CMB maps
  - Planck lensing map
  - External LSS tracers
- The ISW detection with Planck
  - ISW-lensing
  - Cross-correlation with LSS tracers
  - Stacking on the position of large structures
- The ISW map recovery

IFCA Instituto de Física de Cantabria

The ISW with Planck: ISW-lensing

Planck has provided the **1st detection of the ISW by using only CMB data**, via the ISW-lensing bispectrum.

Four different estimators have been applied:

- Cross-angular power spectrum **correlation between the CMB and the lensing potential** maps
- General **bispectrum estimators**, adapted to the ISW-lensing shape (see Bartjan Van Tent and Paul Shellard talks for details):
  - KSW
  - Binned
  - Modal

The ISW with Planck: ISW-lensing

Planck has provided the **1st detection of the ISW by using only CMB data**, via the ISW-lensing bispectrum.

Error bars are derived from coherent simulations, according to the best-fit Planck alone parameters.

Table 2. Amplitudes $A^{T\phi}$, errors σ_A and significance levels of the non-Gaussianity due to the ISW effect, for all component separation algorithms (C-R, NILC, SEVEM, and SMICA) and all the estimators (potential reconstruction, KSW, binned, and modal). For the potential reconstruction case, an additional minimum variance (MV) map has been considered (see Planck Collaboration XVII 2013 for details).

Estimator		C-R		NILC		SEVEM		SMICA		MV	
$T\phi$	$\ell \geq 10$	0.52 ± 0.33	1.5	0.72 ± 0.30	2.4	0.58 ± 0.31	1.9	0.68 ± 0.30	2.3	0.78 ± 0.32	2.4
	$\ell \geq 2$	0.52 ± 0.32	1.6	0.75 ± 0.28	2.7	0.62 ± 0.29	2.1	0.70 ± 0.28	2.5		
KSW		0.75 ± 0.32	2.3	0.85 ± 0.32	2.7	0.68 ± 0.32	2.1	0.81 ± 0.31	2.6		
binned		0.80 ± 0.40	2.0	1.03 ± 0.37	2.8	0.83 ± 0.39	2.1	0.91 ± 0.37	2.5		
modal		0.68 ± 0.39	1.7	0.93 ± 0.37	2.5	0.60 ± 0.37	1.6	0.77 ± 0.37	2.1		

This ISW-lensing bispectrum induces **a bias on local f_{NL} of around 7**.

The ISW with Planck: ISW-lensing

Planck has provided the **1st detection of the ISW by using only CMB data**, via the ISW-lensing bispectrum.

Error bars are derived from coherent simulations, according to the best-fit Planck alone parameters.

Consistency check →

Table 3. For each pair of estimators we provide the mean difference among the amplitudes estimated from the data ($\Delta A^{T\phi}$), the dispersion of the differences between the amplitudes estimated from the simulations (s_A), the ratio of this dispersion to the larger of the corresponding sensitivities (η), and the correlation coefficient (ρ).

		KSW	binned	modal
$T\phi$	$\Delta A \pm s_A$	-0.11 ± 0.10	-0.21 ± 0.21	-0.07 ± 0.21
	η	0.32	0.56	0.56
	ρ	0.95	0.84	0.84
KSW	$\Delta A \pm s_A$		-0.10 ± 0.19	0.04 ± 0.19
	η		0.52	0.51
	ρ		0.86	0.87
binned	$\Delta A \pm s_A$			0.14 ± 0.15
	η			0.41
	ρ			0.92

IFCA Instituto de Física de Cantabria

The ISW with Planck: cross-correlation with LSS tracers

Correlation with surveys has been studied with three statistics:

Cross-angular power spectrum

$$\hat{C}_\ell^{\mathrm{TG}} = \frac{1}{2\ell+1}\sum_{m=-\ell}^{+\ell} t_{\ell m} g^*_{\ell m}$$

Cross-correlation function

$$\hat{C}^{\mathrm{TG}}(\theta) = \frac{1}{N_\theta}\sum_{i,j} T_i G_j,$$

$$C^{\mathrm{TG}}(\theta) = \sum_{\ell=0}^{\ell_{\max}} \frac{2\ell+1}{4\pi} C_\ell^{\mathrm{TG}} P_\ell(\cos\theta)$$

Covariance wavelets coefficients

$$\hat{\Omega}^{\mathrm{TG}}(R) = \frac{1}{N_{\mathrm{pix}}}\sum_i \omega_{\mathrm{T}_i}(R)\,\omega_{\mathrm{G}_i}(R)$$

$$\Omega^{\mathrm{TG}}(R) = \sum_{\ell=0}^{\ell_{\max}} \frac{2\ell+1}{4\pi} C_\ell^{\mathrm{TG}} \omega_\ell^2(R)$$

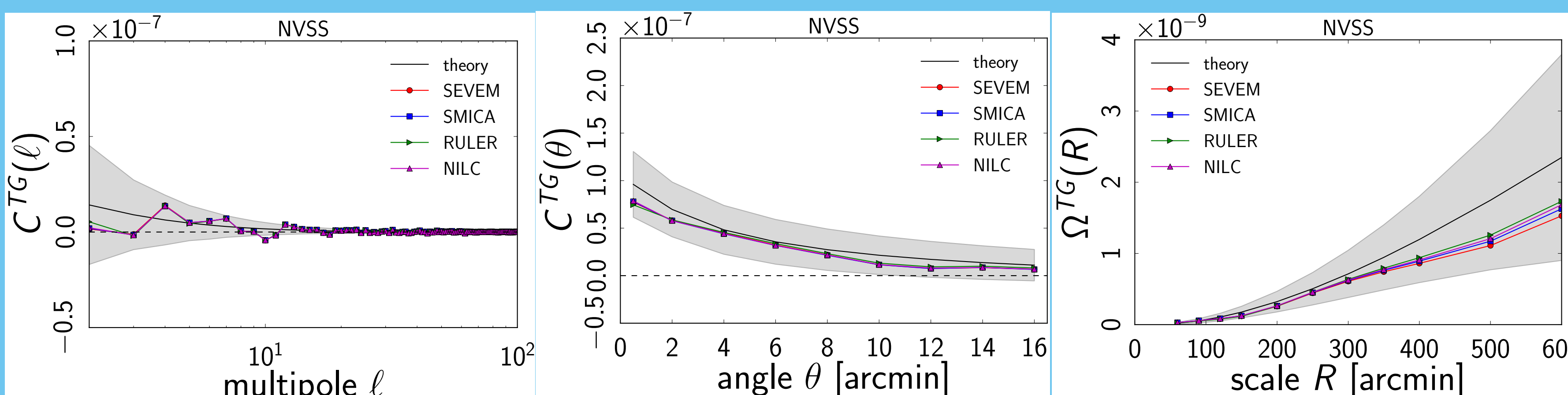

The ISW with Planck: cross-correlation with LSS tracers

As an example: the **covariance of the SMHW coefficients** for the **4 CMB clean maps**, and the **3 LSS surveys**.

Error bars are derived from coherent simulations, according to the best-fit Planck alone parameters.

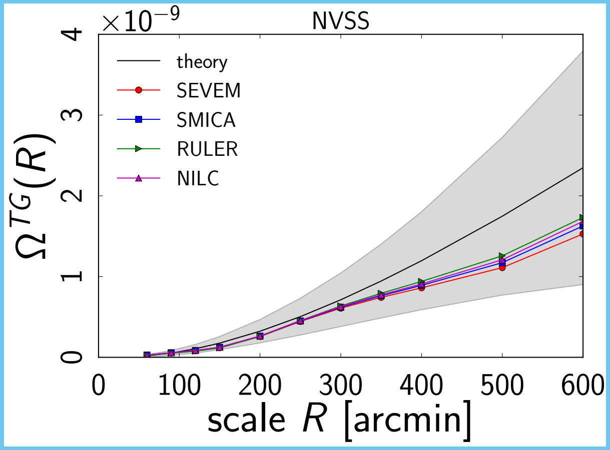

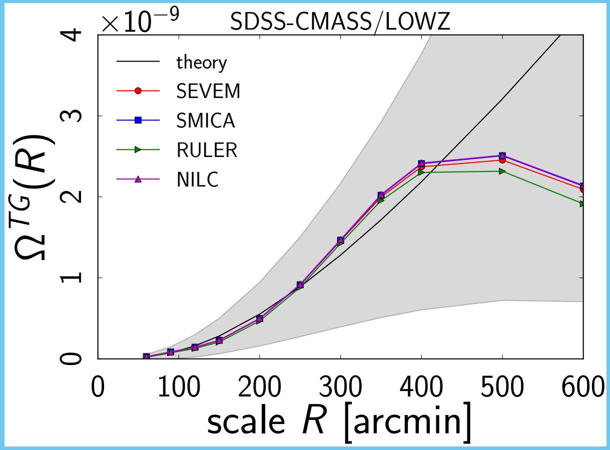

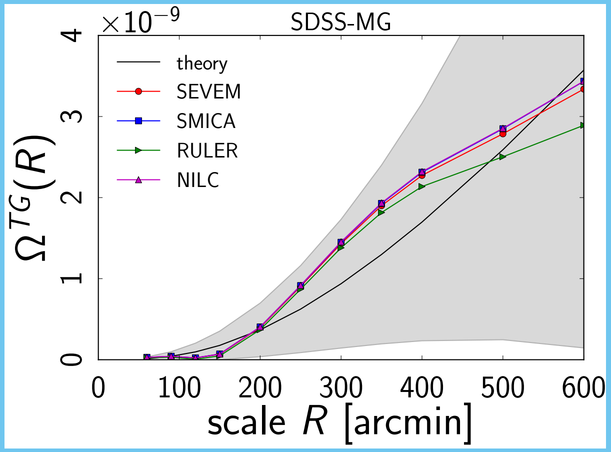

The ISW with Planck: cross-correlation with LSS tracers

Table 6. Amplitudes A, errors σ_A and significances A/σ_A of the CMB-LSS cross-correlation (survey by survey and all together) due to the ISW effect, for all component separation algorithms (C-R, NILC, SEVEM, and SMICA) for the CAPS, CCF, and SMHWcov estimators.

LSS data	$\hat{\xi}_a^{xy}$	C-R		NILC		SEVEM		SMICA	
NVSS	CAPS	0.86 ± 0.33	2.6	0.91 ± 0.33	2.8	0.90 ± 0.33	2.7	0.91 ± 0.33	2.7
	CCF	0.80 ± 0.33	2.4	0.84 ± 0.33	2.5	0.83 ± 0.33	2.5	0.84 ± 0.33	2.5
	SMHWcov	0.89 ± 0.34	2.6	0.93 ± 0.34	2.8	0.89 ± 0.34	2.6	0.92 ± 0.34	2.7
SDSS-CMASS/LOWZ	CAPS	0.98 ± 0.52	1.9	1.09 ± 0.52	2.1	1.06 ± 0.52	2.0	1.09 ± 0.52	2.1
	CCF	0.81 ± 0.52	1.6	0.91 ± 0.52	1.8	0.89 ± 0.52	1.7	0.90 ± 0.52	1.7
	SMHWcov	0.80 ± 0.53	1.5	0.89 ± 0.53	1.9	0.87 ± 0.53	1.6	0.88 ± 0.53	1.7
SDSS-MG	CAPS	1.31 ± 0.57	2.3	1.43 ± 0.57	2.5	1.35 ± 0.57	2.4	1.42 ± 0.57	2.5
	CCF	1.00 ± 0.57	1.8	1.11 ± 0.57	2.0	1.10 ± 0.57	1.9	1.10 ± 0.57	1.9
	SMHWcov	1.03 ± 0.59	1.8	1.18 ± 0.59	2.0	1.15 ± 0.59	2.0	1.17 ± 0.59	2.0
all	CAPS	0.84 ± 0.31	2.7	0.91 ± 0.31	2.9	0.88 ± 0.31	2.0	0.90 ± 0.31	2.9
	CCF	0.77 ± 0.31	2.5	0.83 ± 0.31	2.7	0.82 ± 0.31	2.6	0.82 ± 0.31	2.7
	SMHWcov	0.86 ± 0.32	2.7	0.92 ± 0.32	2.9	0.89 ± 0.32	2.8	0.91 ± 0.32	2.9

The ISW with Planck: cross-correlation with LSS tracers

Consistency check

Table 5. For each pair of estimators we provide the mean difference among the amplitude estimations (ΔA), the dispersion of these differences (s_A), the ratio (η) of this dispersion to the expected sensitivity (i.e., the inverse of the signal-to-noise numbers given in the last column of Table 4), and the correlation coefficient (ρ).

		CCF	SMHWcov
CAPS	$\Delta A \pm s_A$	-0.01 ± 0.12	0.06 ± 0.07
	η	0.36	0.21
	ρ	0.93	0.98
CCF	$\Delta A \pm s_A$		0.08 ± 0.14
	η		0.42
	ρ		0.92

The ISW with Planck: cross-correlation with LSS tracers

- As expected, most of the signal comes from NVSS
- As happens with the ISW-lensing, the actual value is slightly smaller than the fiducial model
- **Lower detections** than those previously reported from WMAP. Two major reasons:
  - Better agreement between the estimated amplitude and the expected value: 1σ or 2σ vs 0.5σ ➔ catalogues description?
  - Planck Ω_Λ **lower** than WMAP one ➔ "**less ISW effect**" **(~10%)**

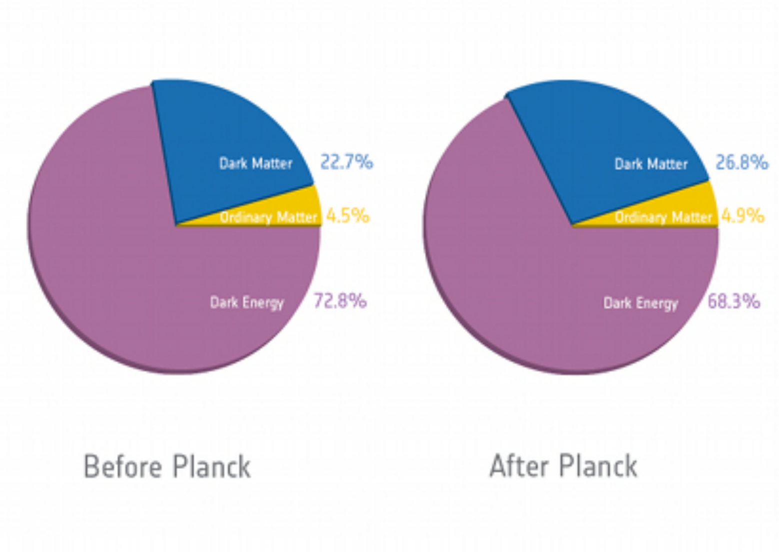

The ISW with Planck: Stacking on the position of large structures

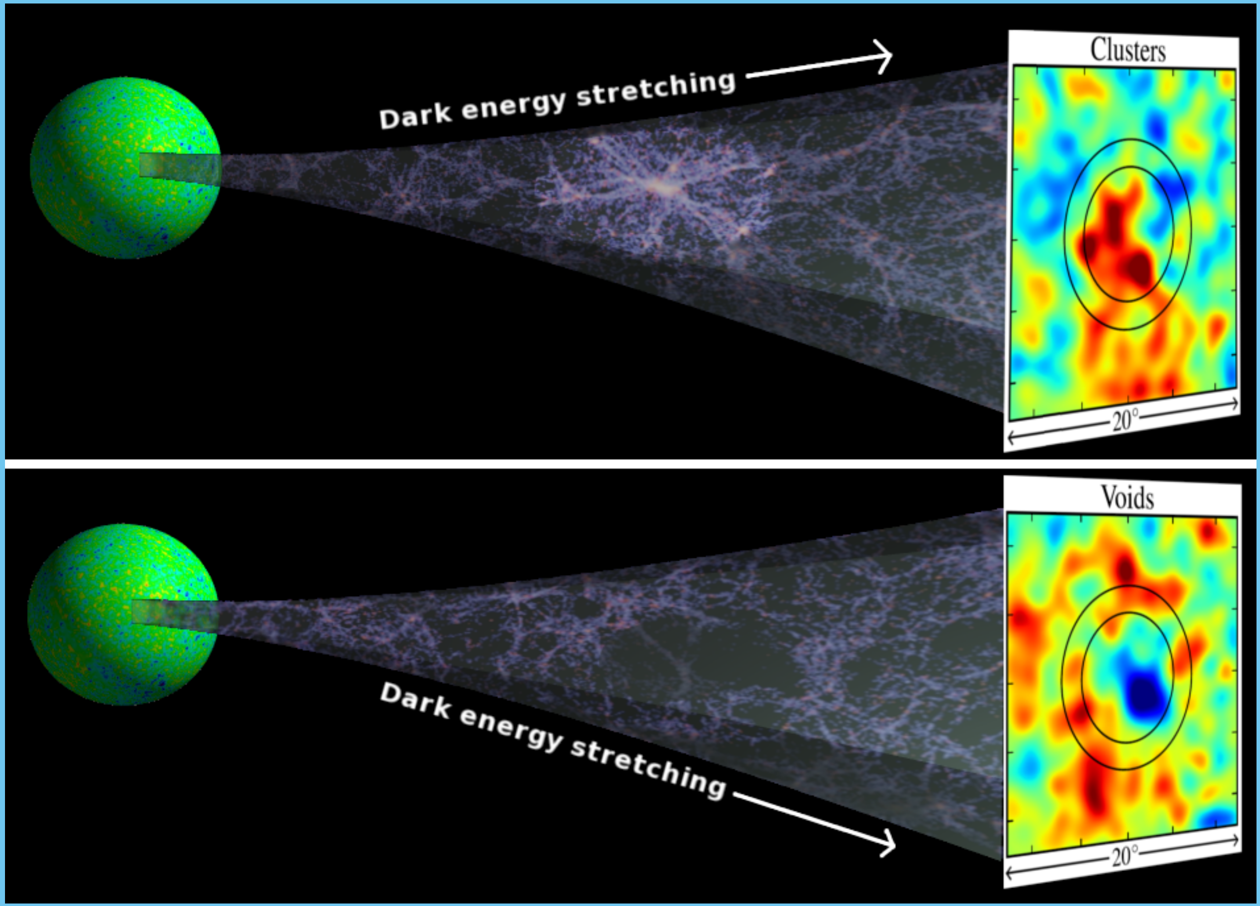

[Granett et al.]

The ISW with Planck: Stacking on the position of large structures

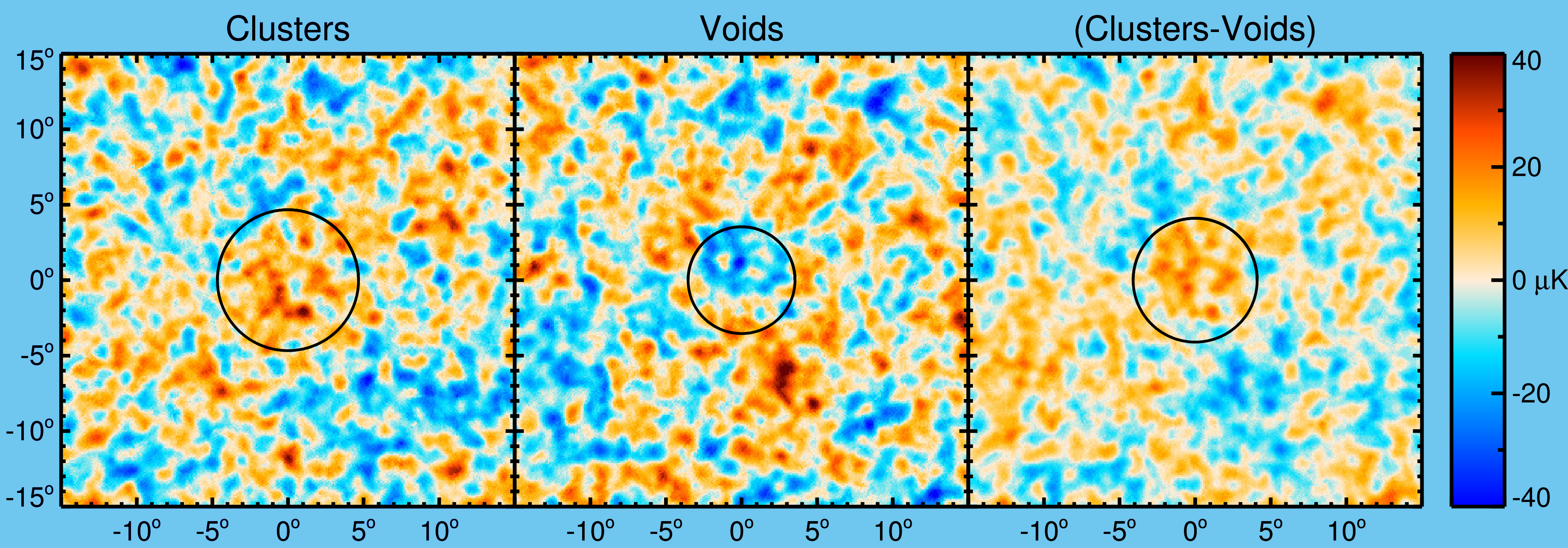

Stacked regions of Planck SMICA map corresponding to the positions of the 50 **superclusters** (left) and 50 **supervoids** (center) of the Grannet et al. 2008 catalogue. Right ➔ **combined** structures. Circles indicate the scale at which the s2n of the photometry is maximal.

The ISW with Planck: Stacking on the position of large structures

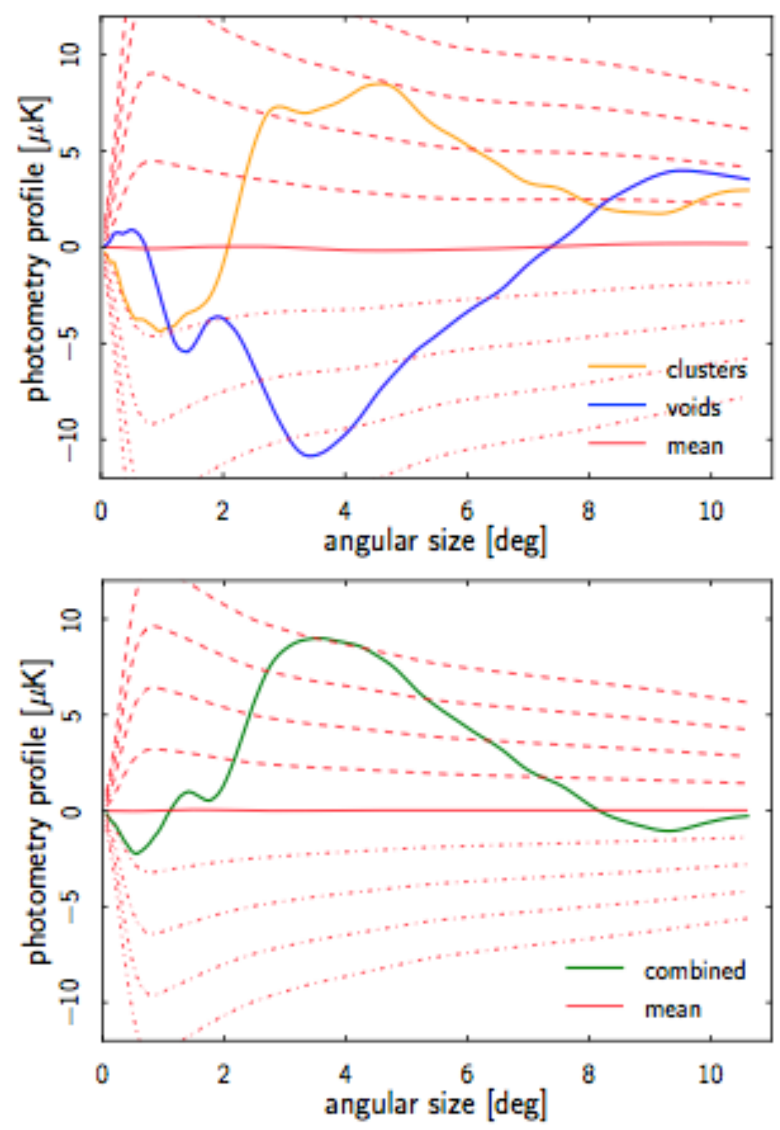

Amplitude and shape of the photometric profile is in tension with the ΛCDM expectations (a factor of 2 at least):

- Max void signal -11.3μK at 3.5° ➔ 3.3σ
- Max cluster signal +8.5μK at 4.7° ➔ 3.0σ
- Max combined signal +8.7μK at 4.1° ➔ 4.0σ

Voids give more signal than clusters, opposite to expectations.

The relative size at which the signal is maximum is 2.6 and 1.3 times the radius of clusters and voids, respectively. Value for clusters seems too large.

Lowest multipole removed from the maps to avoid gradients.

The ISW with Planck: Stacking on the position of large structures

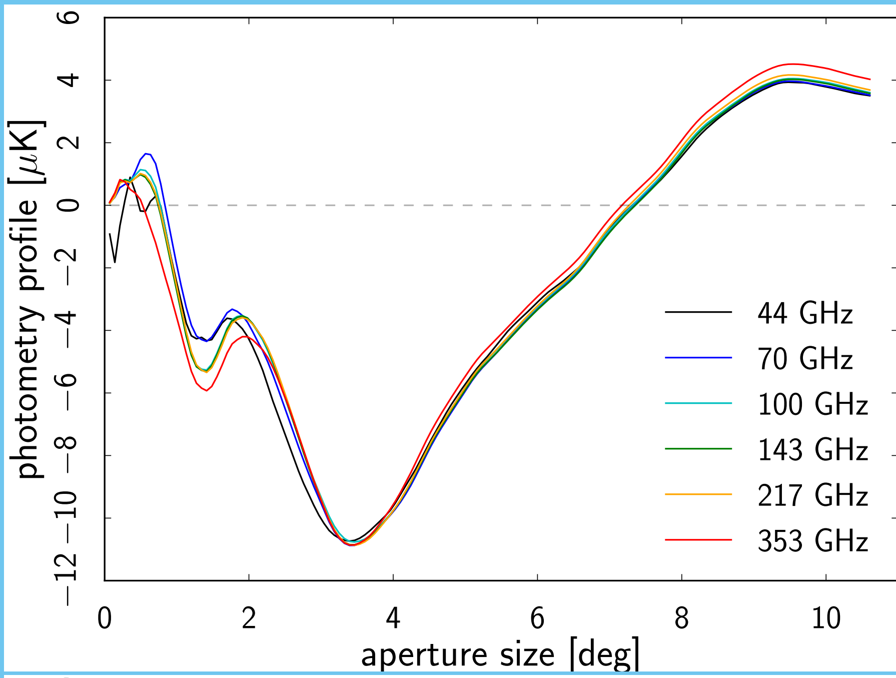

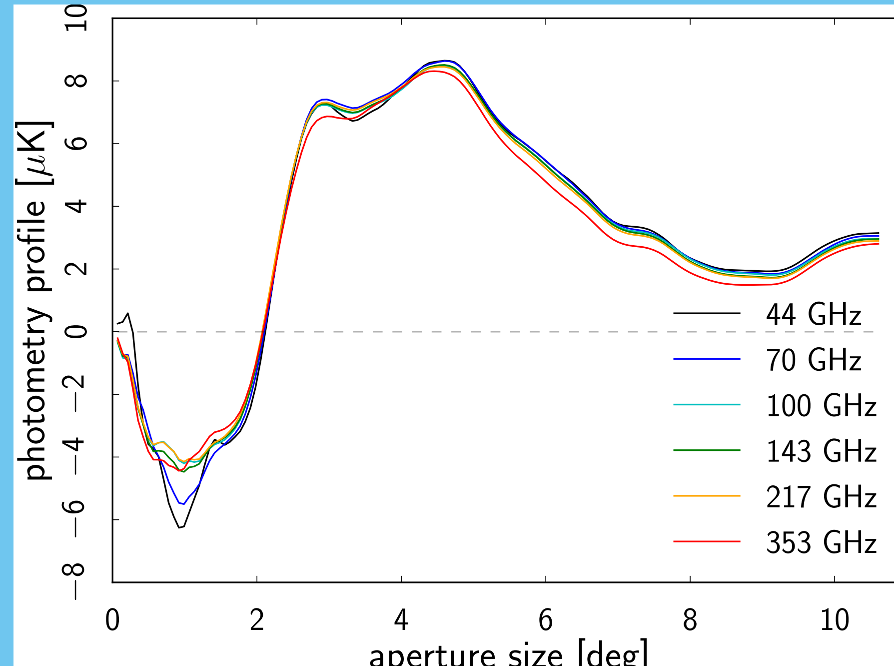

The photometric profiles are studied on the **SEVEM clean maps at frequencies from 44 to 353 GHz**. No significant dependence is observed ➔ **confirmation of the thermal origin of the signal**.

- The data
  - Planck CMB maps
  - Planck lensing map
  - External LSS tracers
- The ISW detection with Planck
  - ISW-lensing
  - Cross-correlation with LSS tracers
  - Stacking on the position of large structures
- **The ISW map recovery**

IFCA Instituto de Física de Cantabria

The ISW map recovery

ISW

CMB

δn

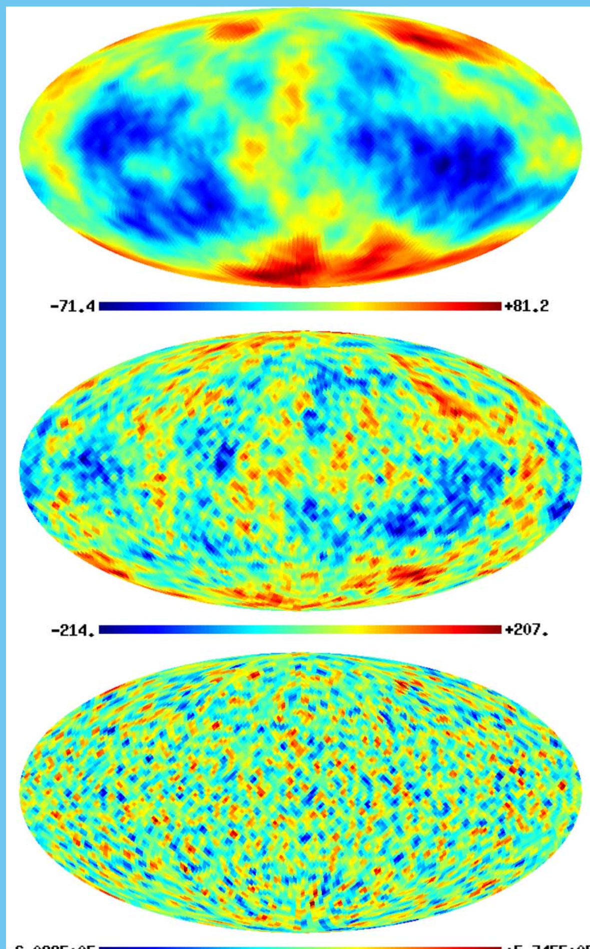

[Barreiro et al. 2008]

rec ISW

Joint filter

rec ISW

Wiener filter

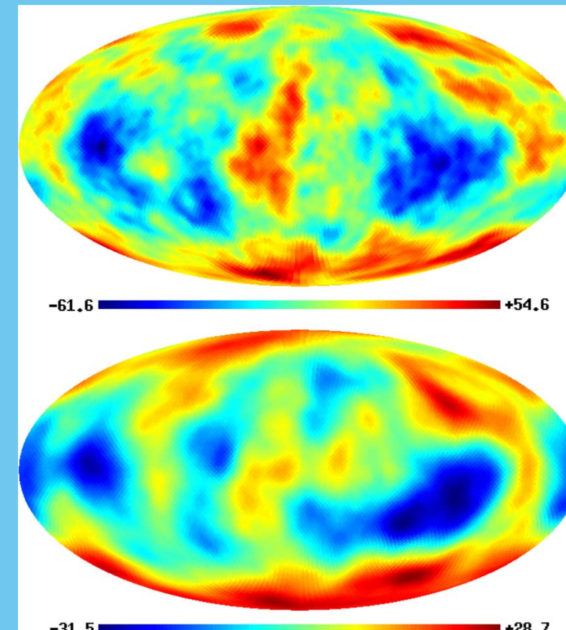

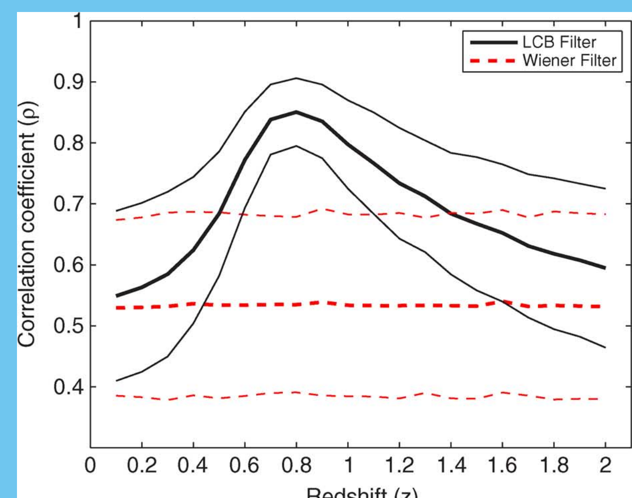

The ISW map recovery

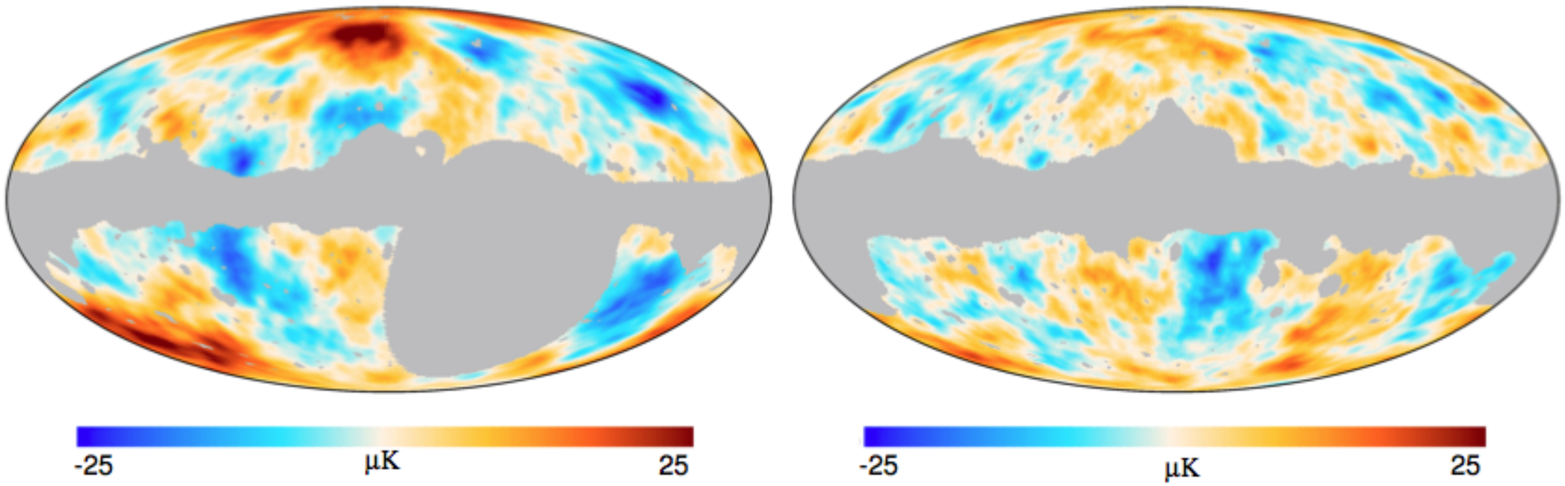

Fig. 11. Reconstructed ISW map from the *Planck* CMB and NVSS data (left) and from the *Planck* CMB and lensing potential maps (right). Note that the maps are not expected to look exactly the same, since each of them provides a partial reconstruction of the noisy ISW signal (see Sect. 6.2 for details).

$$\hat{s}_{\ell m} = \frac{L_{12}(\ell)}{L_{11}(\ell)} g_{\ell m} + \frac{L_{22}^2(\ell)}{L_{22}^2(\ell) + C_\ell^{\mathrm{n}}} \left(d_{\ell m} - \frac{L_{12}(\ell)}{L_{11}(\ell)} g_{\ell m} \right)$$

Recovered ISW

CMB clean map

LSS tracer map

Covariance Matrix

$$\mathbf{C}(\ell) = \begin{pmatrix} C_\ell^g & C_\ell^{sg} \\ C_\ell^{sg} & C_\ell^s \end{pmatrix}$$

$$\mathbf{C}(\ell) = \mathbf{L}(\ell)\mathbf{L}^T(\ell)$$

Cholesky blocks

$$L_{11} = \sqrt{C_\ell^g}, L_{12} = C_\ell^{sg}/\sqrt{C_\ell^g}$$

$$L_{22} = \sqrt{\left|\mathbf{C}(\ell)\right|/C_\ell^g}$$

The ISW map recovery

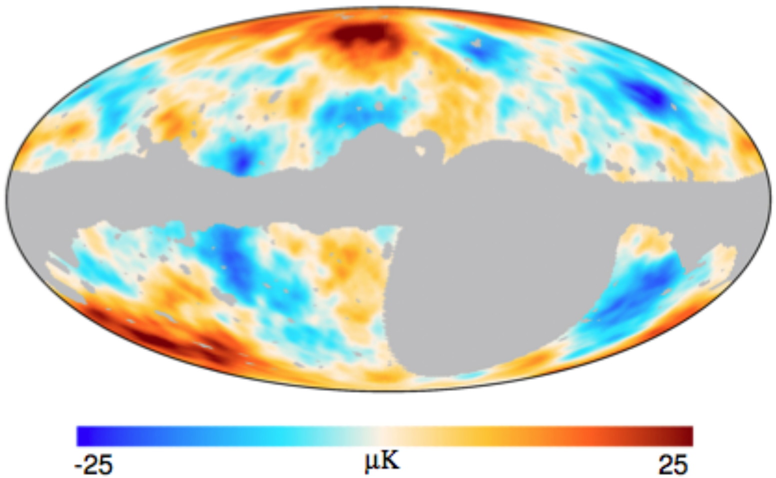

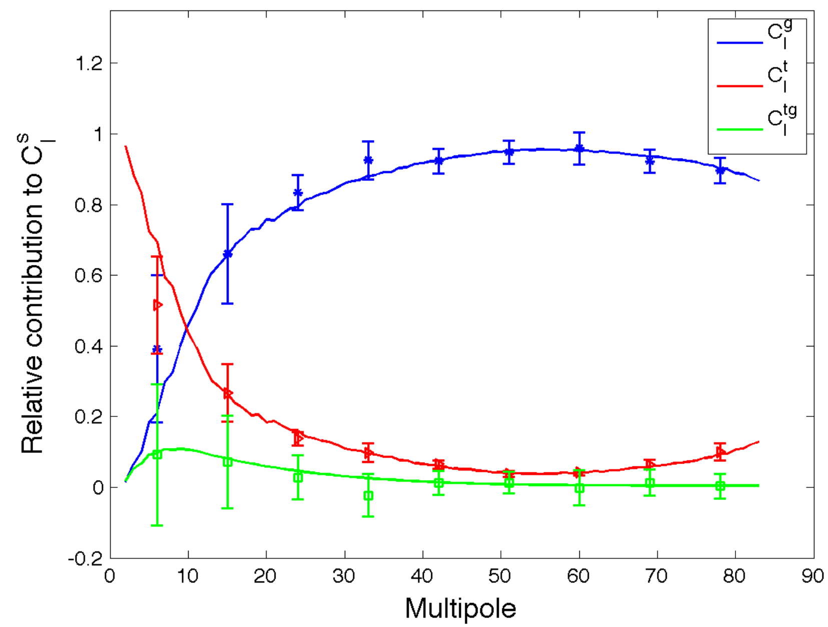

Fig. 11. Reconstructed ISW map from the *Planck* CMB and NVSS (right). Note that the maps are not expected to look exactly the sa noisy ISW signal (see Sect. 6.2 for details).

$$\hat{s}_{\ell m} = \frac{L_{12}(\ell)}{L_{11}(\ell)} g_{\ell m} + \frac{L_{22}^2(\ell)}{L_{22}^2(\ell) + C_\ell^{\mathrm{n}}} \left(d_{\ell m} - \frac{L_{12}(\ell)}{L_{11}(\ell)} g_{\ell m} \right)$$

Recovered ISW

CMB clean map

LSS tracer map

Covariance Matrix

$$\mathbf{C}(\ell) = \begin{pmatrix} C_\ell^g & C_\ell^{sg} \\ C_\ell^{sg} & C_\ell^s \end{pmatrix}$$

$$\mathbf{C}(\ell) = \mathbf{L}(\ell)\mathbf{L}^T(\ell)$$

Cholesky blocks

$$L_{11} = \sqrt{C_\ell^g}, L_{12} = C_\ell^{sg}/\sqrt{C_\ell^g}$$

$$L_{22} = \sqrt{|\mathbf{C}(\ell)|/C_\ell^g}$$

IFCA Instituto de Física de Cantabria

- **Polarization**
- **N-body simulations**
- **Future galaxy surveys**

- Polarization
- N-body simulations
- Future galaxy surveys

Polarization

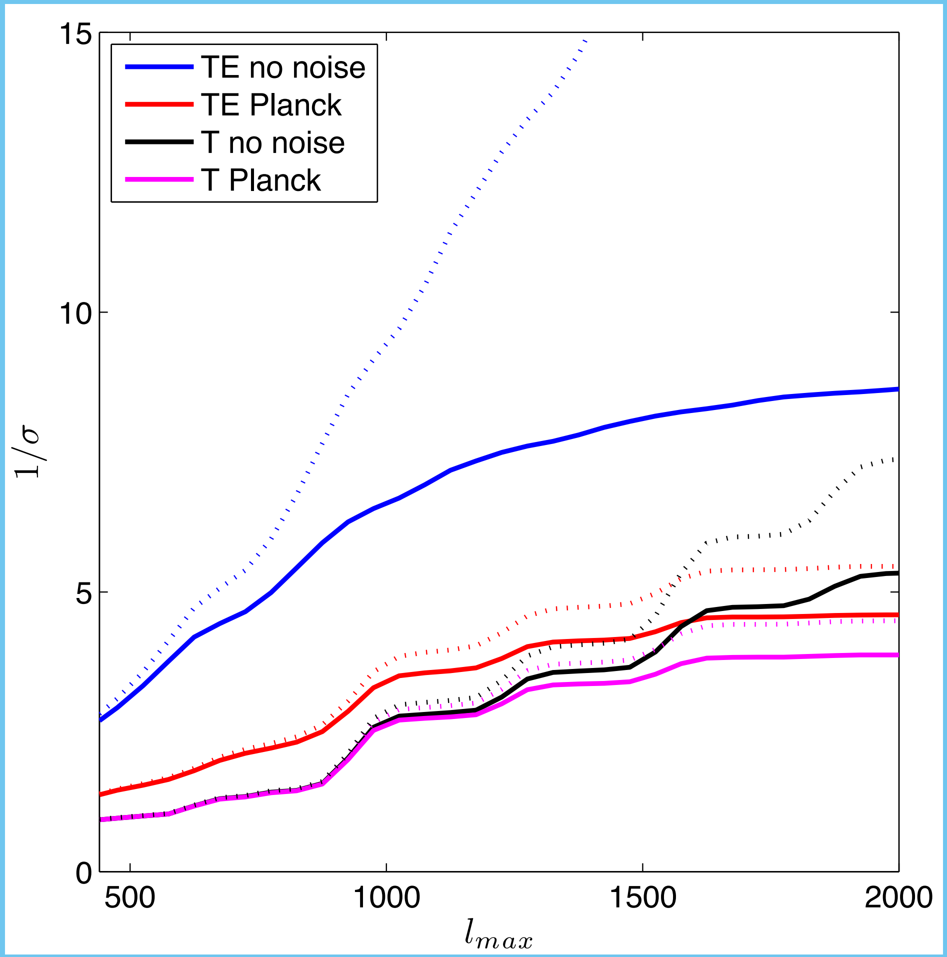

Lewis et al. 2011

The total ISW-lensing could be increased up to **2.9σ** (currently it is 2.5σ), similar to the ISW-LSS cross-correlation.

Multiply by $(f_{sky})^{0.5}$ to take into account the sky coverage

I F C A
Instituto de Física de Cantabria

Polarization

Looking at **stacked Q_r images** on the position of clusters and voids, could help to **understand the anomalous behaviour observed in T** data.

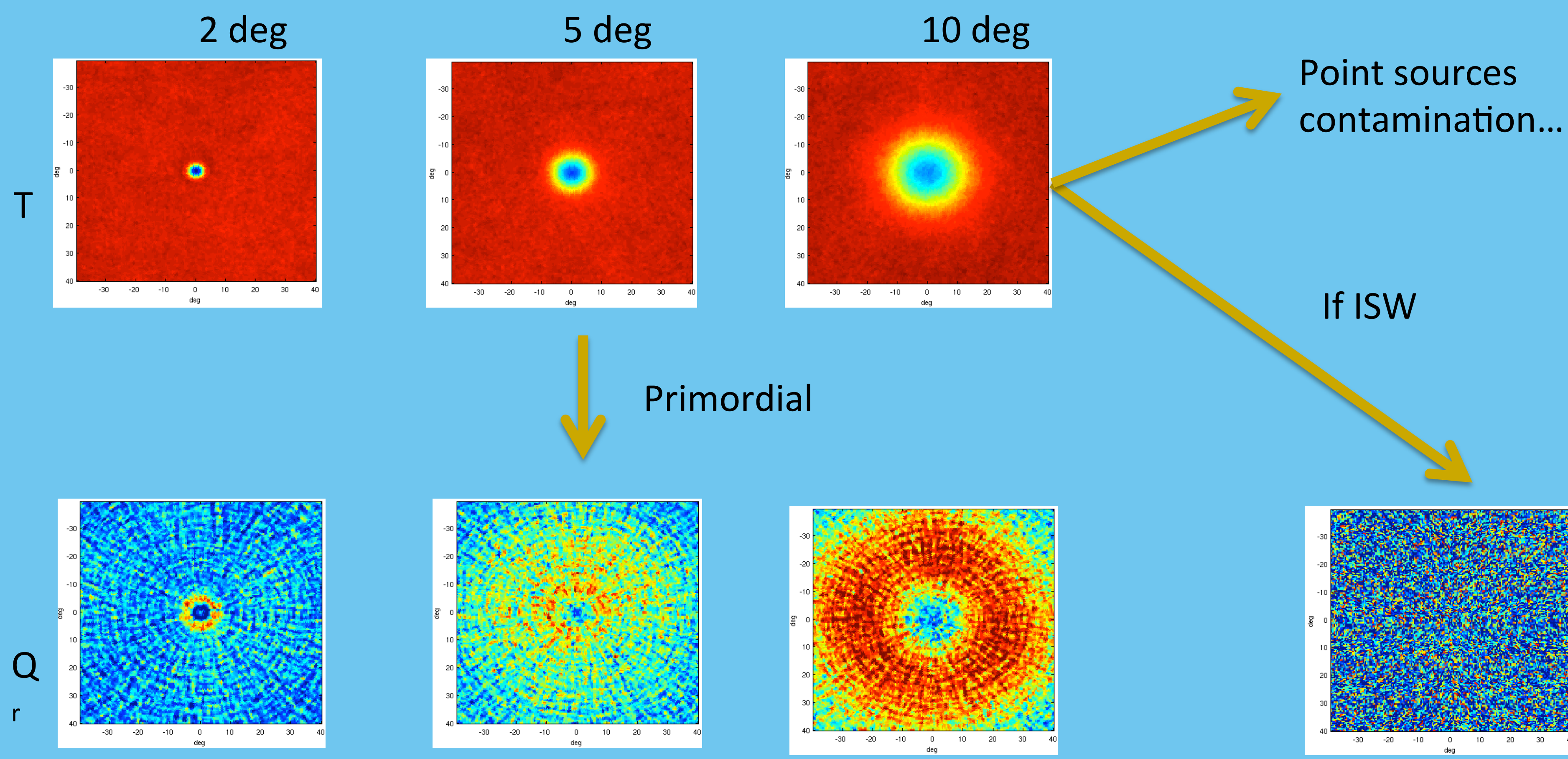

IFCA Instituto de Física de Cantabria

- Polarization
- **N-body simulations**
- Future galaxy surveys

Instituto de Física de Cantabria

N-body simulations

The Jubilee ISW Project I: simulated ISW and weak lensing maps and initial power spectra results

W. A. Watson[1,⋆], J. M. Diego[2], S. Gottlöber[3], I. T. Iliev[1], A. Knebe[4], G. Yepes[4], R. B. Barreiro[2], J. González-Nuevo[2], S. Hotchkiss[5], A. Marcos-Caballero[2], E. Martínez-González[2], S. Nadathur[6], P. Vielva[2]

[1] *Astronomy Centre, Department of Physics & Astronomy, Pevensey II Building, University of Sussex, Falmer, Brighton, BN1 9QH, United Kingdom*
[2] *IFCA, Instituto de Física de Cantabria (UC-CSIC). Avda. Los Castros s/n. 39005 Santander, Spain.*
[3] *Leibniz-Institute for Astrophysics, An der Sternwarte 16, 14482 Potsdam, Germany*
[4] *Departamento de Física Teórica, Modulo C-XI, Facultad de Ciencias, Universidad Autónoma de Madrid, 28049 Cantoblanco, Madrid, Spain*
[5] *Department of Physics, University of Helsinki and Helsinki Institute of Physics, P.O. Box 64, FIN-00014 University of Helsinki, Finland*
[6] *Fakultät für Physik, Universität Bielefeld, Postfach 100131, D-33501 Bielefeld, Germany*

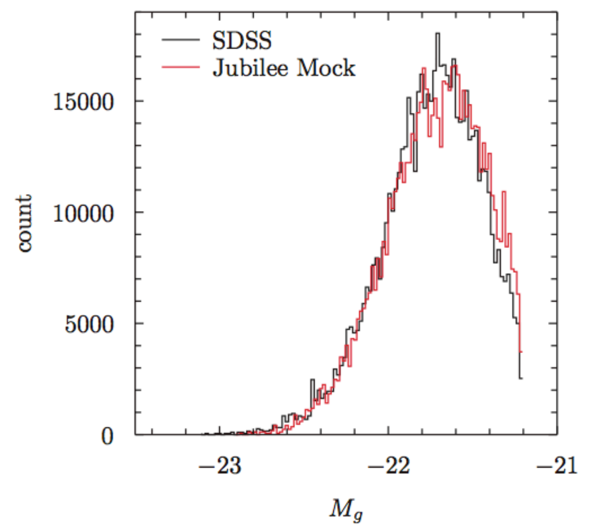

Figure 2. Histogram comparing SDSS LRGs with Jubilee mock LRGs. The full dataset of SDSS DR7 LRGs from Kazin et al. (2010) is plotted together with a random subsample of Jubilee Mock LRGs with the same total number count. The SDSS data is taken from a redshift range of $z = 0.16$ to 0.44 with a g-band absolute magnitude range of $M_g < -21.2$ (calibrated at $z = 0.3$). Jubilee mock data is taken from the $z = 0.3$ output slice.

- $6h^{-1}$ Gpc box
- 216 billion particles
- Covers all the universe from z=1

- **Designed for testing ISW**
  - Correlation with galaxy catalogues
    - **LRGs**
    - **Radio**
  - **Correlation with lensing**
  - **Stacking on the voids and clusters**

N-body simulations

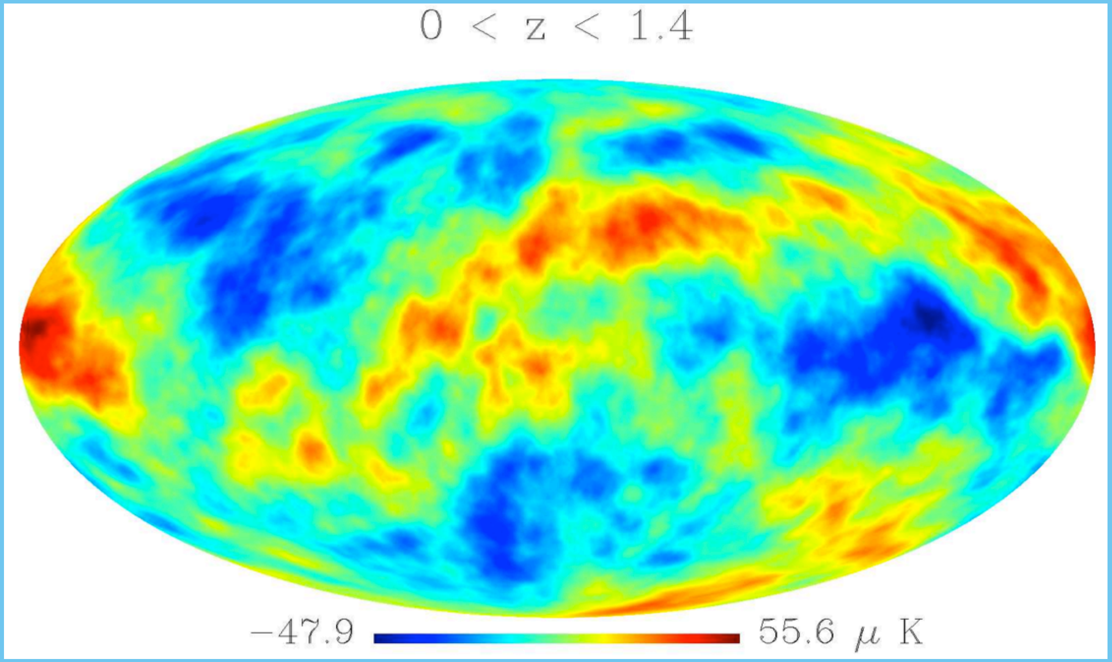

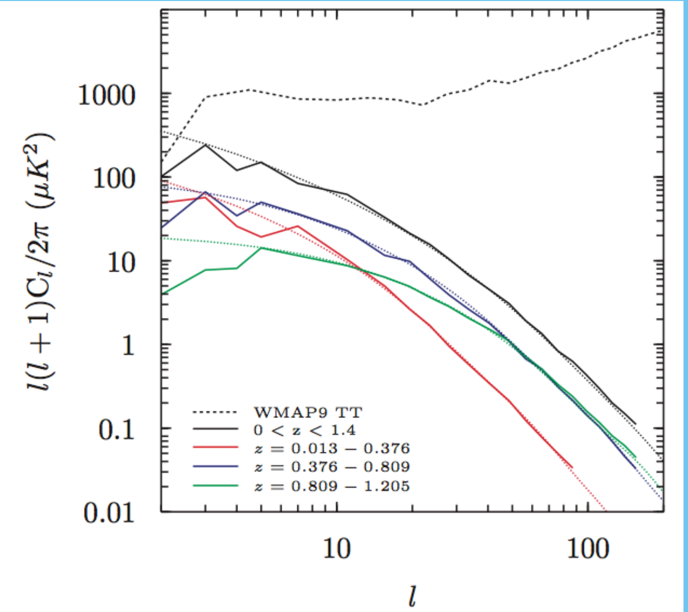

Figure 8. The power spectrum of the temperature anisotropies that arise from the ISW effect. Power from individual redshift bins are shown along with the full integrated ISW effect (from $z = 0$ to 1.4) and the CMB TT power spectrum. Linear theory predictions are shown as dotted lines. The redshift bin widths correspond to those of Figure 7.

N-body simulations

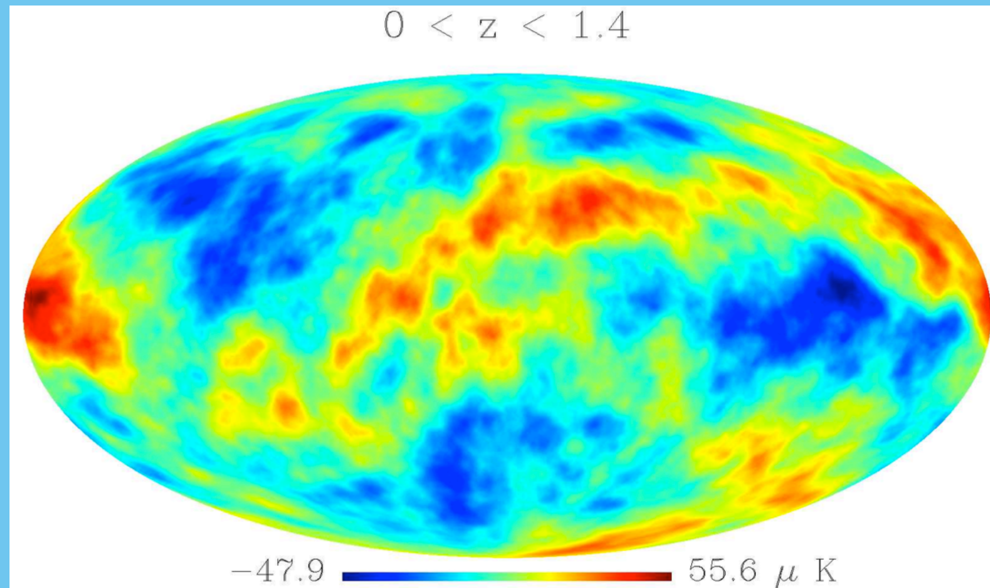

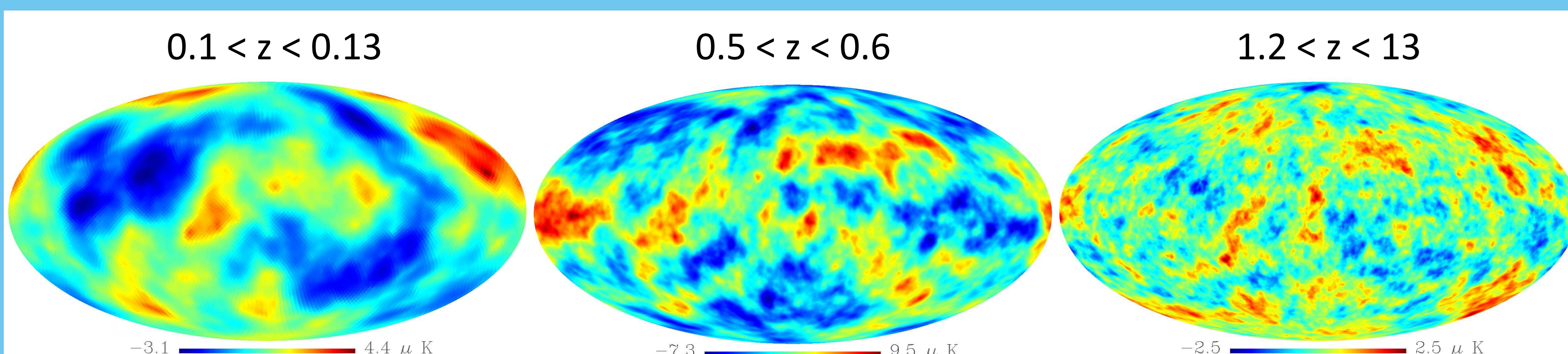

- Polarization
- N-body simulations
- **Future galaxy surveys**

Future galaxy surveys

- The next decade(s) is expected to provide a huge amount of **new data from galaxy surveys**.
- Although primary science is BAOs and weak lensing, **ISW studies can benefit out of some of them**, e.g.:
    - J-PAS
    - BigBOSS
    - PanSTARSS2
    - LSST
    - Euclid
- Expected sky coverage, redshift range and number of galaxies would allow **for ISW detections in [3, 5]σ** ➔ Starting to be useful for DE and modified gravity studies.
- In particular, an **opportunity to explore ISW-QSOs correlations widely**.

- ISW is a **weak signal**
- Current LSS **surveys** allow for 3σ **detections** ➔ **confirmed with Planck**
- Similar limit reachable by **ISW-lensing** (ISW detection with a single experiment) ➔ **made by Planck for the 1st time**
- **Stacking of CMB fluctuations** on the position of LSS features shows un-expected levels of ISW signal ➔ **Planck confirms its thermal nature**
- Planck **polarization** will help **to increase the ISW signal in ~15%** (via ISW-lensing)
- **N-body simulations** very important to **better understand the ISW physics**
- **Future surveys** will allow for **5σ detections**, approaching to the theoretical limit.

The scientific results here presented are a product of the Planck Collaboration, including individuals from more than 1000 scientific institutes in Europe, the USA and Canada

Planck is a project of the European Space Agency, with instruments provided by two scientific Consortia funded by ESA member states (in particular the lead countries: France and Italy) with contributions from NASA (USA), and telescope reflectors provided in a collaboration between ESA and a scientific Consortium led and funded by Denmark.